Fire in open-plan Compartments

Numerical Simulation Models Informed by Small-Scale Fire Tests

Structure Mechanics
Omid Rashidi

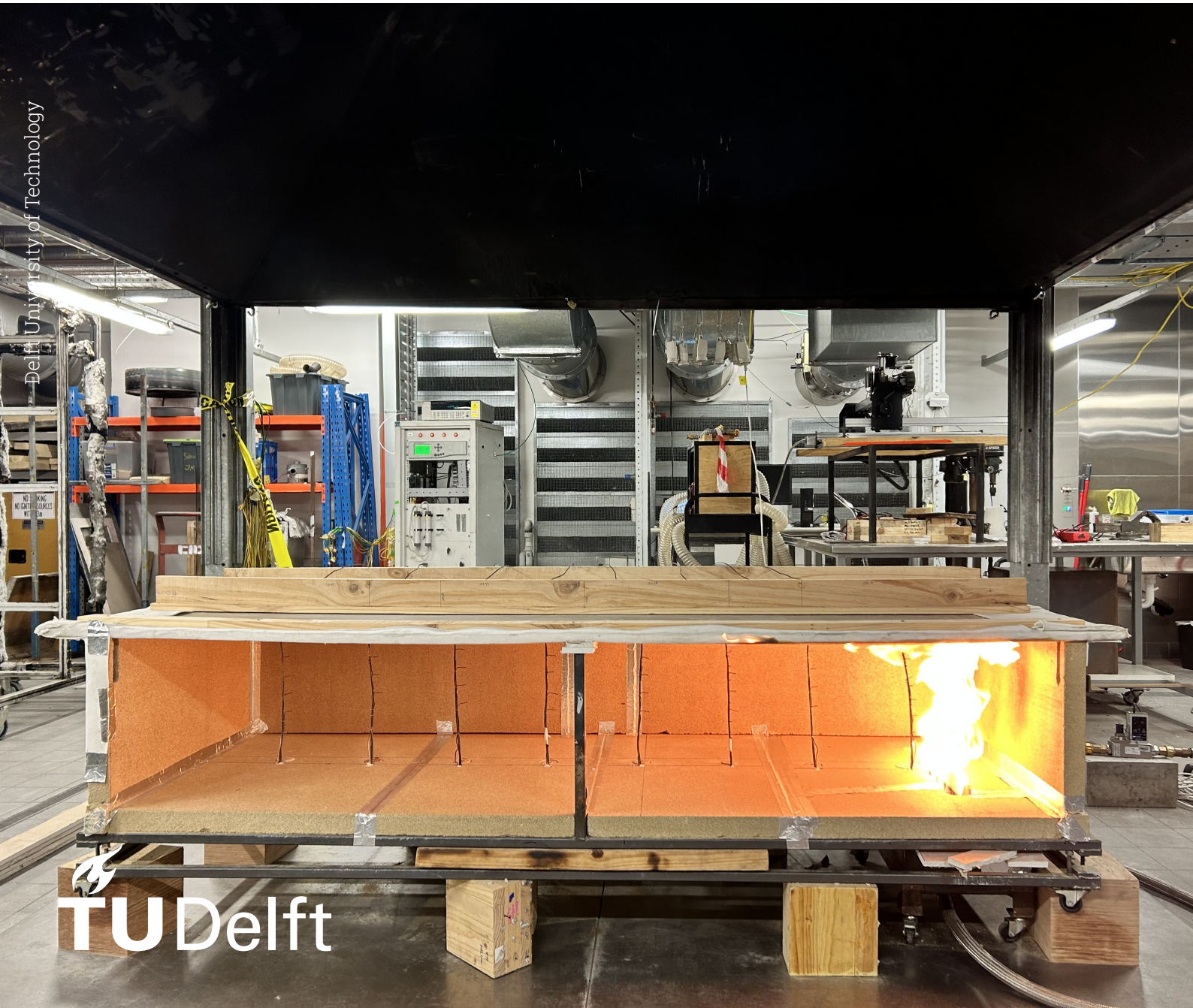

Delft University of Technology

TU Delft

Fire in open-plan Compartments

Numerical Simulation Models Informed by Small-Scale Fire Tests

by

Omid Rashidi

Author

Supervisor:	Dr. Zhuojun Nan
Supervisors:	dr. ir. P. C. J. Hoogenboom and dr. ir. H. R. Schipper
Project Duration:	September, 2025 - October, 2025
Faculty:	Faculty of Civil Engineering and Geosciences, Delft

Cover: Original photo (by Dr. Zhuojun Nan)
Style: TU Delft Report Style, with modifications by Daan Zwaneveld

TU Delft

Preface

At the end of the Bachelor of Civil Engineering in Delft University of Technology, I, Omid Rashidi, undertook this project as my Bachelor thesis.
This report is useful for those seeking guidance on fire dynamics in open-plan compartments and their simulations.
Hereby, I would like to thank my supervisor Dr. Zhuojun Nan for her constant support and guidance during the project. In addition, I would like to thank dr. ir. P. C. J. Pierre Hoogenboom and dr. ir. H. R. Roel Schipper for offering their support and interest.

Omid Rashidi
Delft, October 2025

Summary

Modern urban environments are characterised by buildings with open-plan compartments. However, the behaviour and spread of fire in such spaces remains a subject that is not fully understood and warrants continued investigation. Full-scale fire test can provide valuable insights on fire behaviour, but are rarely conducted due to their high costs, environmental impact and destructive nature. Consequently, reduced-scale fire tests are preferred as a feasible alternative. Since complete scaling in fire science is unattainable, partial scaling is applied when interpreting results from reduced-scale fire tests. Nevertheless, large numbers of reduced-scale fire test is also not practical, as they remain costly and resource-intensive. Fire Dynamics Simulator (FDS) numerical models offer a cost-efficient and practical solution to these challenges, providing an alternative means to study fire behaviour without financial and logistical limitation of physical experiments.

The objective of this study is to develop numerical simulation models, informed and supported by reduced-scale fire experiments conducted in open-plan compartments. These experiments are part of a study, which investigates fire dynamics in open-plan spaces, through reduced-scale testing with compartment geometry of 2.22 m x 0.80 m x 0.40 m. The case study experiment features no edge beam, leaving one side of the compartment fully open. A propane gas burner functions as combustion source and the walls, ceiling and floor of the compartment are constructed of fire-resistant materials. The instrumentation utilised consists of thermocouples distributed throughout the compartment, to measure temperature over time, and thin skin calorimeters on both ceiling and the floor to record heat flux variations. The relevant results of this is the table with average temperature measurements provided in Appendix D.

In order to assess the validity of FDS numerical models to replicate the experiment results - at least in terms of phenomenological similarities, because replication of exact numerical values is not attainable - four models with progressively refined mesh resolutions and other parametric enhancements are considered in this study. The models use identical geometric configuration as the reduced-scale experiments and employ the same propane combustion source with heat release rate of 90.4 kW. The mesh size in the first model was set to 0.04 m, which is considered coarse in this context. The second model utilised a finer mesh of 0.025 m, resulting in a noticeable improvement in the agreement between predicted average temperatures and the experimental outcomes. Further refinement of mesh toward 0.018 m led to an even closer correspondence to the experimental results. At this stage, for efficiency considerations, the mesh domain was reduced in size to only include the compartment boundaries. The final simulation incorporated multiple parametric enhancements. First, the mesh size was refined to 0.01 m, at which the model was assumed to have reached grid-independence. Second, is the adjustment of fuel release mechanism from heat release rate per unit area (HRRPUA) to mass loss rate formulation, which enabled the model to more accurately represent the experimental conditions. The third is enhancements in inherent material properties of the compartment model, which better reflect the materials used in the experiment. In the final simulation, the mesh was divided into 26 regions, with finer resolution near the burner area to enhance accuracy while maintaining computational efficiency. Although the final simulation incorporated considerable enhancements, the results did not converge towards the experimental outcomes as strongly as anticipated. This may be attributed to the fact that the grid-independence has already been achieved, which had been the primary source of improvement in the earlier simulations. Nevertheless, if the results are evaluated in terms of phenomenological trends and overall similarities, it can be concluded that FDS simulations are capable of reproducing experimental behaviour with reasonable approximation, thereby providing valuable insights into the underlying processes. This is particularly encouraging, because there still is room for improvements in the simulations. Future research could focus on refining material properties - such as thermal conductivity and density - or on improving the representation of ventilation conditions to improve model performance. Moreover, extending the simulation duration-time and collecting larger number of data points can improve the reliability of the results.

Contents

Preface i

Summary ii

Nomenclature iv

1 Introduction 1
- 1.1 Motivation . . . 1
- 1.2 Objective . . . 2
- 1.3 Structure . . . 2

2 Experiment and Data 3
- 2.1 Background . . . 3
- 2.2 Experimental Results . . . 4

3 FDS Simulation and Methodology 6
- 3.1 Set up . . . 6
- 3.2 Simulations . . . 7
- 3.3 Output Results . . . 8
- 3.4 Validation . . . 9

4 Discussion 11
- 4.1 Key Findings and Interpretation . . . 11
- 4.2 Connection to Existing Literature . . . 12
- 4.3 Modelling Lessons . . . 12
- 4.4 Strengths and Limitations . . . 12

5 Conclusion and Recommendation 13

A Source Code Example 14

B Planning 16

C References 17

D Average temperature table 18

E Table of Simulation Temperature Results 19

F Temperature Results Visualisation 20

G FDS File 21

Nomenclature

Abbreviations

Abbreviation	Definition
ISA	International Standard Atmosphere

Symbols

Symbol	Definition	Unit
T	Temperature	[$^{\circ}$C]
HRR	Heat release rate	[kW]
$HRRPUA$	Heat release rate per unit are	[kW/m^2]
ρ	Density	[kg/m^3]
ε	Emissivity	[$-$]
k	Thermal conductivity	[W/mK]
C	Specific heat capacity	[kJ/kgK]

1

Introduction

1.1. Motivation

Fire in buildings claim many lives and cause enormous amounts of economic damage each year. Although the threat of fire-spreading has always existed in urban areas and communities, with increasing urbanism throughout the world and cities getting ever more crowded, this threat has never been more acute. In order to get a vivid picture of the scale of this threat, it is important to point to the relevant statistics, for example, over 350,000 house fires occur annually and there are more than $ 48 billion in property losses each year in the US (RainbowRestoration, 2025). There are also individual cases where fire spread have caused enormous damage, both in terms of life and property. An important case to mention would be the Grenfell Tower Fire in London (figure 1.1), where in a tragic midnight on June 14th 2017, a fast spreading fire in the 24-storey building claimed more than 70 lives (Wikipedia, 2025).

Fire spread in open-plan compartments is a concept that is not fully within grasp as of yet. Most traditional fire behaviour models for open-plan compartments are based on assumptions that simplify fire behaviour, leading to different predictions than real-life outcomes. One of these simplifications is the assumption of uniform fire burning throughout the entire compartment, while inspections have shown that fire tends not to burn simultaneously throughout the entire compartment, but tends to travel across the floor or even vertically to other floors, resulting in a limited area in fire at any one time (Jamie Stern-Gottfried & Guillermo Rein, 2012). Given the shortcomings in fire models and the prevalence of open-plan spaces in modern urban buildings, developing a comprehensive understanding of this phenomenon is essential. However, the advancement of knowledge in this area presents several challenges. The biggest challenge would be that full-scale fire tests tend to be very expensive and destructive, as test materials cannot be reused. In addition, such tests are pretty harmful to the environment as a result of the release of large amounts of greenhouse gases. Consequently, small-scale fire tests present a much more practical alternative, providing valuable insights through controlled investigation with reduced cost. To strengthen the reliability of such experiments, their findings can be validated through fire dynamics simulations, providing robust data that better reflect real-world fire behaviour. Nevertheless, it important to remember that these reduced-scale test still have shortcomings. One limitations that needs to be considered, when it comes to drawing insights from small-scale fire tests is the scaling problem. When using the reduced-scale models, a lot of parameters concerning fire dynamics can be proportionately reduced, for example the heat release rate or compartment geometry. However, this scaling does not apply to parameters such as momentum or time, which also affect fire dynamics (Sam Nothard et al, 2022). Consequently, preservation of all non-dimensional groups governing fire dynamics in not possible, which lead to a complete scaling of fire tests unattainable. Even so, partial scaling remains a practical and valuable approach for investigating phenomenological similarities and general fire behaviour. Therefore, reduced-scale fire tests are utilised to systematically examine specific mechanisms and trends, rather than reproducing full-scale fire dynamics quantitatively. That being said, it is also not feasible to conduct very many reduced-scale fire tests, because even in small proportions, such tests remain destructive and expensive. For that reason, conducting fire dynamics

simulations offer a viable solution, because it enables the exploration of many different scenarios without significant costs. By incorporating data from real fire tests, numerical simulations make it possible to study a wide range of parametric conditions, enabling comprehensive analyses and helping to fill gaps in existing research.



Figure 1.1: Grenfell Tower Fire (Wikipedia, 2025).

1.2. Objective

The main objective of this study is to establish a Fire Dynamics Simulator (FDS) numerical simulation corresponding to an experimentally observed fire scenario in an open-plan compartment. The project aims to examine how FDS can replicate the spatial and temporal fire developement, temperature distribution, and environmental conditions observed during the experiment. Through this comparative analysis, the study seeks to enhance understanding of the modelling capabilities and limitations of FDS when applied to complex compartment fire phenomena.

1.3. Structure

The project starts with a literature review on fire dynamics and existing fire tests, including both large-scale and small-scale fire tests in order to understand fire spreading behaviour in open-plan compartments and its relevant components. Subsequently, the motivation and the objectives of the project are presented in the introduction at the beginning of the report. This is followed by a detailed discussion of the empirical experiment, which serves as the basis and support for the subsequent simulations. Using the FDS software PYROSIM, a corresponding simulation is developed and executed, and the resulting data is analysed and compared with the experimental measurements in chapter 3. Chapter 3 also includes the validation section, which investigates the suitability of using FDS simulations reproduce experimental fire tests.

2

Experiment and Data

2.1. Background

The study, of which the experiments are a part of, investigates fire dynamics in open-plan compartments by means of reduced-scale testing (2.22 m × 0.80 m × 0.40 m), and serves both as supporting information and a case study for the numerical simulations presented in this work. The series of 1/8-scale tests is designed to represent full-scale fire tests such as the Malveira Fire Test and Veselí Travelling Fire Test. Because it is impossible to preserve all scaling laws in fire science, the reduced-scale experiments are designed to observe phenomenological similarities with the full-scale tests, rather than exact physical outcomes. Hence, when analysing the results, greater emphasis is placed on broader trends in the data, rather than on specific numerical values. The floor and walls of the compartment were constructed from vermiculite board, which is a fire-resistant material. The vermiculite has a density of 375 kg/m^3, a specific heat capacity of 0.94 kJ/kgK, and a thermal conductivity of 0.12 W/mK measured at 200°C (Sam Nothard et al., 2022). For the first three tests, the ceiling of the compartment were "constructed with 16 mm thick plasterboard (with a density reported by the manufacturer of 780 kg/m^3, specific heat capacity of 1.09 kJ/kgK a thermal conductivity of 0.24 W/mK; all at ambient conditions) covered in 5 mm thick ceramic wool (Superwool Paper Insulation) on the exposed surface (ceramic wool with a density of 96 $kg/m3$, a specific heat capacity of 1.13 kJ/kgK, and a thermal conductivity of 0.09 W/mK at 400 $^\circ$C)" (Sam Nothard et al., 2022, p. 3).

There are two main factors that vary in the test condition. First, the heat release rate (HRR) examined at 22.6, 30.1, 37.7, 60.3, 90.4 kW. The second is the placement of an edge beam at the compartment opening, which reduces the opening height from 400 to 340, 290, 220 or 170 mm. The edge beam significantly affect the heat release and distribution within the compartment. As temperature accumulates at higher elevations inside the compartment, heat becomes trapped, resulting in an overall increase in compartment temperature. Furthermore, edge beams affect oxygen availability, thereby impacting the combustion processes occurring within the compartment.

The instrumentation in the test setup was designed to capture different temperature distributions under various conditions. First of all a propane-fuelled line burner was placed on one end of the compartment at an opening on the floor, that released combustible gas. The heat release rate (HRR)(kW), could be predetermined by the burner. A total of 16 thin skin calorimeters (TSCs) were used (8 on the ceiling and 8 on the floor) to measure the heat flux(kW/m^2) on the ceiling and the floor. For monitoring of temperature distribution, eight thermocouple trees, each tree consisting of seven inconel at different heights, were placed inside the compartment. Details of the thermocouple locations and setup can be found in Figure 2.2.

It is important to note that no additional combustible material, like timber were used in the experiments. The reason for it is that the study focuses on analysing fire spread through parameters such as temperature, ventilation and heat flux. Fire propagation is quick, when the surrounding temperature is high and when the heat flux is high enough, surrounding combustible objects can start to ignite on their own. These relationships demonstrate that parameters like temperature and heat flux are strong

indicators of fire development. Therefore, by investigating their behaviour and spatial distribution in open-plan compartments, valuable insights can be gained into the potential dynamics of fire spread in such environments-without incurring the significant costs associated with the fire tests that involve extra combustible materials.

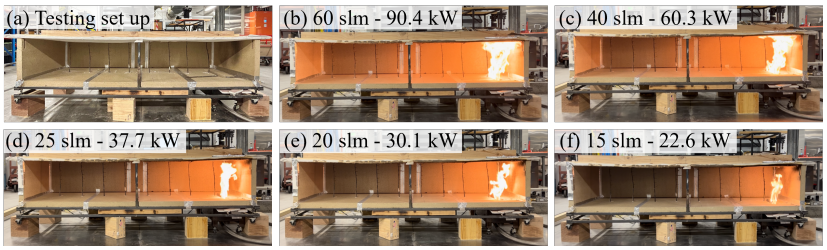

Figure 2.1: Experiment setup.

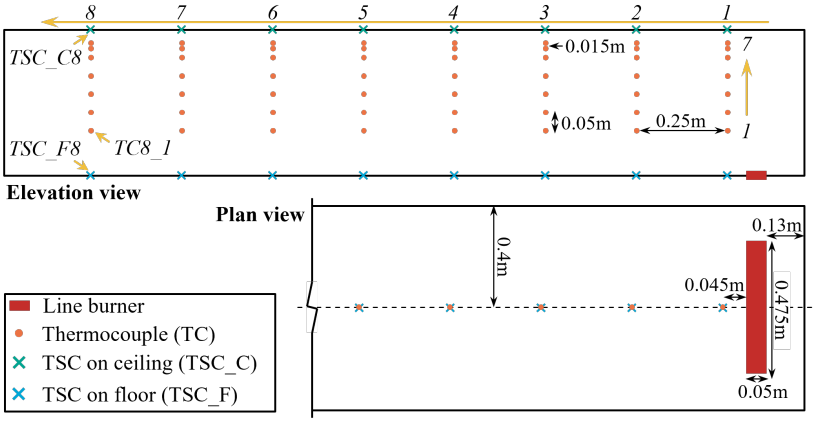

Figure 2.2: Layout of the sensors

2.2. Experimental Results

The experiment was carried out five times, each with different heights of the edge beam, in order to examine its effects on the compartment temperature. Table 2.1 gives a clear oversight about these tests. The results are presented in 5 sets of graphs, with each set consisting of 8 plots, showing the temperature at a location by means of thermocouples, over a 15-minute interval. In each graph, 7 curves represent the temperature readings of each thermocouple. In it important to note however, that the 15-minute duration of the experiments is chosen to ensure that temperature conditions inside the compartment reach its steady-state. This means that when replicating the experiments by means of numerical simulation, the duration of the simulations can be determined by the time it takes to reach the steady-state, which often much less than 15 minutes. Figure 2.3 gives an illustration of the graphs obtained by the experiment without an edge beam. Additionally, Appendix D provides a table summarising the average temperatures measured by thermocouples during the 15-minute experiment without an edge beam, namely test 1.

The results of the experiment indicate that the presence of edge beams, which reduce the opening area of the compartment, has a significant effect on the compartment temperature. This effect is likely related to the influence of ventilation on the fire, as restricted openings can limit oxygen supply and affect combustion behaviour. Additionally, the introduction of edge beams alters temperature profile within the compartment. Heat naturally rises, but the edge beams at the top of the opening partially trap hot gases, leading to heat accumulation over time. This effect is evident in the experimental results, which show that larger edge beams correspond to higher temperatures. Furthermore, the right side of the compartment is consistently hotter, consistent with the location of the fire.

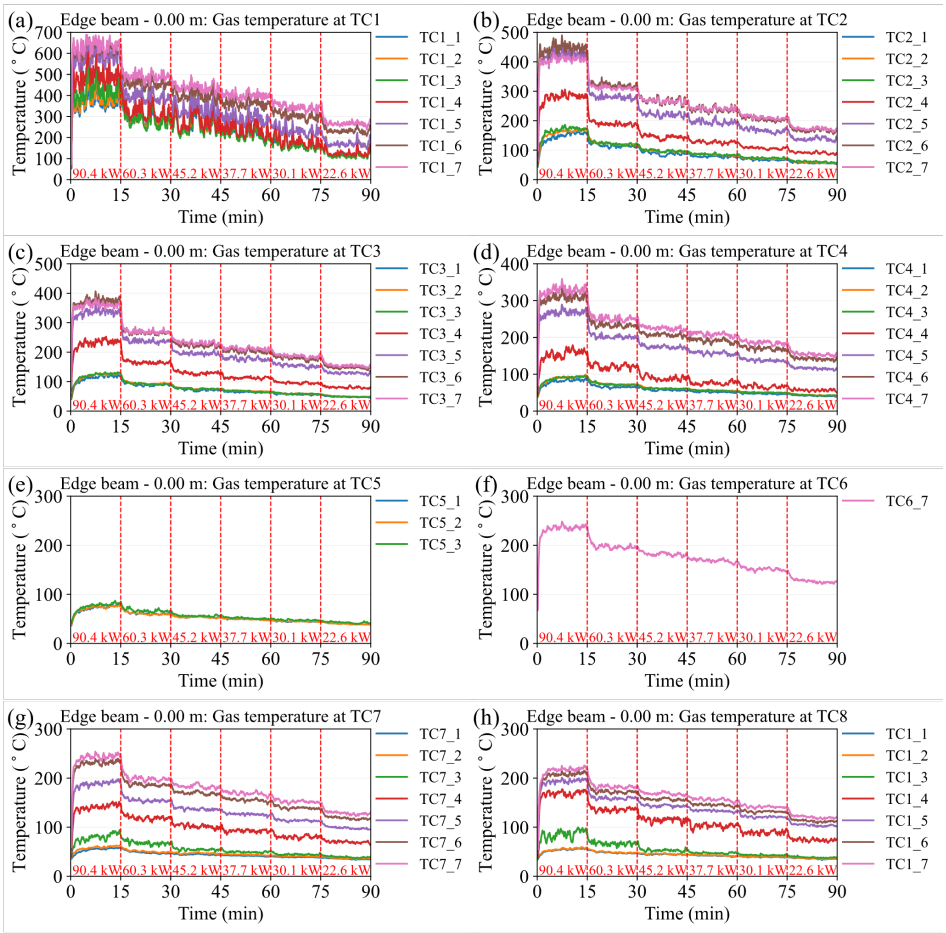

Test1: Edge beam – 0 m

Figure 2.3: Experiment results for setup with no edge beam (test number 1)

Test number	Height of the edge beam (mm)	Height of the opening (mm)	Heat release rate (kW)
1	0	400	22.6, 30.1, 37.7, 60.3, 90.4
2	60	340	22.6, 30.1, 37.7, 60.3, 90.4
3	110	290	22.6, 30.1, 37.7, 60.3, 90.4
4	180	220	22.6, 30.1, 37.7, 60.3, 90.4
5	230	170	22.6, 30.1, 37.7, 60.3, 90.4

Table 2.1: Tests with different fire and ventilation conditions

3

FDS Simulation and Methodology

3.1. Set up

Multiple Pyrosim simulations has been set up with different mesh sizes in order to investigate the compartments condition under different resolutions. The floor and walls of the compartments modelled with vermiculite board, while the ceiling and edge beams are set to be non-combustible plasterboard, which is consistent with the empirical experiment. The compartment has dimensions 2.2 m in length, 0.8 m in width, and 0.4 m in height. For the fire source, a burner is set on one side of the compartment that provides heat at a predetermined rate.

A critical aspects of the FDS simulation is the determination of an appropriate mesh size through a mesh sensitivity study. In this type of study, same simulations are conducted using different mesh sizes, and the convergence in results are analysed. If the simulation outcomes remain consistent with finer resolutions of mesh, the model is considered to be grid-independent (Ricardo Gasparini, 2022). Obtaining an optimal mesh size is a process on its own. Initially, one can acquire an estimation of the mesh size by the FDS mesh size calculator (Andrea, 2021). The calculation employs Formula 1 to obtain the characteristic fire diameter, which primarily depends on the heat release rate associated with the test simulation. Subsequently, for a fine mesh resolution, the cell size is obtained by dividing the characteristic fire diameter D by 16, and the results are summarised in table 3.1.

$$D = \frac{Q}{\rho\, c_p\, T\, \sqrt{g}}^{2/5} \tag{1}$$

Where:

- D = The characteristic fire diameter (m)
- Q = Heat release rate (kW)
- ρ = Air density (1.204 kg/m^3)
- c_p = Air specific heat (1005 $kJ/kg * K$)
- T = Ambient Temperature (293.15 K)
- g = The gravitational constant (9.81 m/s^2)

It is important to note that mesh sizes summarised in table 3.1 are not necessarily the optimal mesh sizes. In order to determine the optimal mesh sizes, multiple simulations with varying mesh resolutions will be conducted, and the resulting data will be assessed to see whether grid-independence has been achieved. The outcomes with also be compared with the corresponding empirical measurements in order to analyse their accuracy and realism. Through this validation process, the final mesh size will be validated. The selected mesh resolution could subsequently be employed in further parametric investigations, in which the compartment would be tested under a wide range of parametric conditions.

HRR	Mesh size (in m)
90.4 kW	0.023
60.3 kW	0.019
37.7 kw	0.016
30.1 kw	0.015
22.6 kW	0.013

Table 3.1: Mesh sizes for different HRR

This approach enables the collection of a more comprehensive dataset and facilitates the examination of the system from different perspectives.

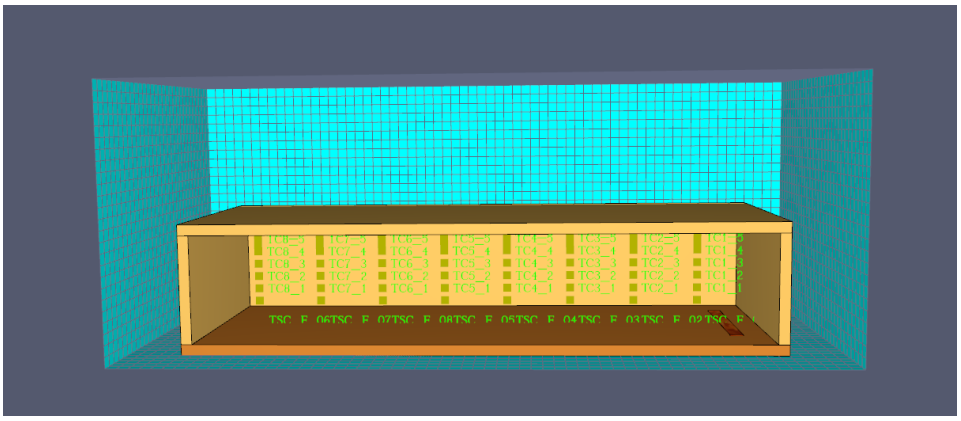

Figure 3.1: Compartment model of the first simulation with coarsen meshes and thermocouple's location

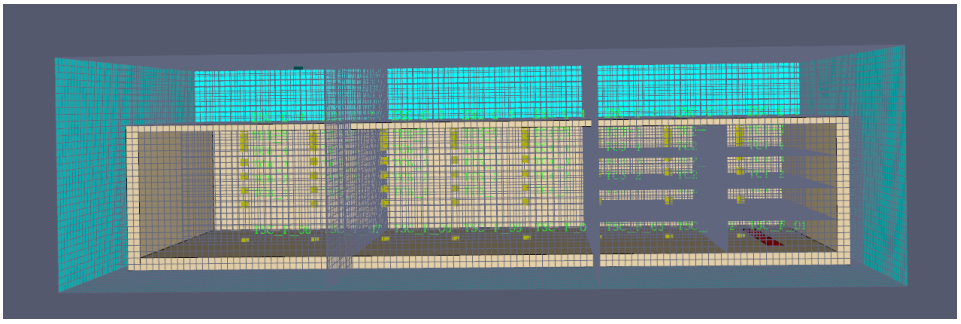

Figure 3.2: Compartment model of the fourth simulation with refined meshes in the fire region

3.2. Simulations

A total of four simulations were conducted in order to examine the effects of the mesh resolution in capturing the accurate temperature distribution. Aside from variations in material properties, all the simulation were conducted using identical parameters, including the heat release rate of 90.4 kW and the same compartment geometry (without an edge beam). It is important to note that parameters such as time-duration and the number of data-points that were adjusted in different simulations. The reason for this change was the heavy nature of the simulations and the long time it would take to conduct a simulation of around five minutes. Hence, for the purposes of feasibility, the time-duration of the experiment were set to a relatively low amount, with the minimum of 30 seconds and a maximum of 140 seconds. Although the relatively low amount of time-duration could be a reason why the obtained data would be less accurate, however the graphs which show the temperature progressions as a function of time, illustrated that the compartment reaches a steady-state temperature relatively soon after the ignition of fire. From this follows that although the low time-duration affects the accuracy of the results, this effect is not great, considering the steady-state situation inside the compartment.

The first simulation model was conducted using mesh size of 0.04 m, which is a relative coarse mesh resolution for this model. The material properties of the compartment were defined as *inert* (a detailed explanation is provided later), and the fuel release mechanism was modelled using heat release rate per unit area (HRRPUA) approach. The mesh size in the second model was refined to 0.025 m, while keeping all other parameters in the simulation model unchanged. This refinement led to slight, but noticeable improvements in the results(further discussed in the next section). The third model employed a finer mesh of 0.018 m, and in this case the mesh domain boundaries were reduced, as the original domain was unnecessarily large and no significant activity occurred beyond the compartment area. The enhanced mesh resolution led to even more promising data at this point. Conducting the fourth simulations, additional adjustments were made in the parameters of the simulation, in an attempt to achieve greater accuracy in the results. These adjustments include, aside from the finer mesh of 0.01 m, the method of specifying the fuel supply from heat release rate per unit area (HRRPUA), expressed in kW/m^2, to using the mass loss rate, expressed in $kg/m^2 * s$. It is anticipated that by specifying the fuel supply in terms of mass loss rate, the released propane gas becomes independent of its density. This is an advantageous approach, because gas density varies with temperature, which would otherwise lead to different amounts of combustible material being released under different thermal conditions. Simultaneously, the material properties in the compartment model were refined to better capture heat reflection effects of the walls and ceiling and contribute to a more realistic dataset. These material properties include, thermal conductivity ($W/(m * K)$), mass density (kg/m^3), specific heat capacity ($J/(kg * K)$) and thermal emissivity (-), which are adjusted to match the values specified in the experiment data. Finally, to reduce the overall computation time of conducting the simulations - since the simulations require a considerable amount of time to run - the compartment is divided into regions with different mesh densities. A finer mesh is applied in the fire source and plume region to capture detailed fire dynamics accurately, while coarser meshes are used in areas farther from the fire to reduce computational cost and improve simulation efficiency. Taken together, these suggest that the closer alignment of the gathered data with the empirical data is not only due to the higher mesh resolution, but also additional refinements in the overall model (more on this in the next section).

After conducting each simulation, the gathered data output is collected in the form of an Excel-file, which then is visualised via Python. Appendix F provides a graphical representation of the temperature variation over time. The codes for calculating the average temperature measured by each thermocouple is written in such a way that it takes into account only the steady-state region.

3.3. Output Results

The output results of the four simulations conducted in order to investigate the feasibility of reproducing the experiment results is summarised in table 3.2. One thermocouple from each thermocouple tree is selected from each simulation and compared with the experiment result of the corresponding thermocouple for their average temperature measurement. The results show that when the mesh resolution increases, the results steadily approach the experiment measurements. This is surely the case for the majority of the thermocouple results, however some results do show considerable discrepancies in their convergence to the experimental results. Although the primary focus is on the behavioural trends of compartment temperature, the magnitude of the differences in final average temperature values is sufficiently large to suggest that there must be an underlying issue within model the requires resolution. It is unlikely that these discrepancies stem from coarsen mesh size, as grid independence is expected to have been achieved with a cell size of 0.01 m. This suggests that there are other factors in the numerical model that do not accurately replicate the experimental conditions. One possible factor could be the underdevelopment of the simulation results, which may arise from conducting simulations for insufficient time-duration or collecting suboptimal amount of data points. These limitations stem primarily from the absence of sufficient computation power, which causes certain simulations to require excessive amounts of time to complete, thereby making it simply impractical to conduct large amounts of simulations. Another possible reason is the potential inadequacy of the material properties selected for the model. The refinements in material properties in the fourth (last) simulation includes the adjustment of inherent properties of the walls, ceiling and the floor to better reflect the experimental conditions, as these were first set to the default setting of *Inert*. *Inert* is a standard FDS surface property in which the surface temperature always remains at the ambient temperature (Thunderhead Engineering, 2025). In addition, based on the literature, the default value of emissivity of solid surfaces is set to be 1.0 (Kevin

	TC1_7	TC2_7	TC3_7	TC4_7	TC5_3	TC6_7	TC7_7	TC8_7
Mesh size (in m)								
0.04	1095	1025	877	704	42	455	405	390
0.025	919	825	668	503	26	348	330	311
0.018	863	715	563	477	23	315	295	273
0.01	927	797	697	547	80	349	292	263
Experiment results	**614**	**402**	**354**	**304**	**77**	**234**	**241**	**215**

Table 3.2: Average temperature in °C captured by thermocouples with different mesh resolutions

B. McGrattan et al., 2001), which means that the surface reflects 100% of the incident thermal radiation. In the fourth simulation, the material properties were adjusted as follows: specific_heat = 1.13 kJ/kgK, conductivity = 0.09 W/mK, density = 96 kg/m^3, and emissivity = 0.9 (-). These values are consistent with the experimental data, which is reported in *Factors influencing the fire dynamics in open-plan compartments with an exposed timber ceiling*. (Nothard et al., 2022). From this, it can be concluded that emissivity of the compartment surfaces are not responsible for the observed discrepancy in the results. Whether other properties such as, thermal conductivity or density contribute to the differences between simulation and experiment results remains unknown and should be the focus of future studies.

Nevertheless, it is essential to keep in mind that the primary objective of these simulations is to identify phenomenological similarities and trends between the simulations results and the experimental measurements, rather than to achieve exact numerical agreements. In this context, it is reasonable to conclude that phenomenological similarities were observed between simulation results and the experimental measurements in terms of their average temperature. Moreover, the accuracy of these results are expected to increase as the models are further refined, including enhancements in other material properties and adjustments in various software-related parameters, such as simulation duration and number of data points.

3.4. Validation

When validating whether FDS simulations are useful for predicting fire behaviour in open-plan compartments in term of phenomenological similarities, it is important to consider several key criteria. The first thing to consider, is whether there are any recognisable trends in the data obtained by the simulations and the measurements gathered by the experiment. In this regard, there are recognisable trends in the approximation of the experiment results. First is the steady convergence of the simulation data points towards the experimental results. In this area, although noticeable discrepancies remain between the numerical and experimental results, these differences tend to decrease through subsequent simulations with improved boundary and modelling conditions. As the refinement of the simulations reaches grid independence with a mesh size of 0.01 m, further improvements must be sought in other parameters like material properties (thermal conductivity or density), fuel related properties or ventilation condition. It is anticipated that with enhancements in these parameters, the difference could even be further reduced. Another key trend to observe is the average temperature distribution along the length and height of the compartment. This behaviour is best illustrated in graph 3.3, which presents the average temperature recorded by thermocouples positioned in different height and longitudinal location. The result show that the highest average temperature occurs on the right side of the compartment - corresponding to the burner location - while the lowest temperature appear in the left side. Additionally. the data presented in Appendix E , reveal a progressive increase in average temperature with elevation, which is also consistent with the experimental observations. Although this behaviour might seem self-evident, it is important to emphasize it, as it represents an fundamental aspect of the phenomenological similarity between the experimental and simulation results.

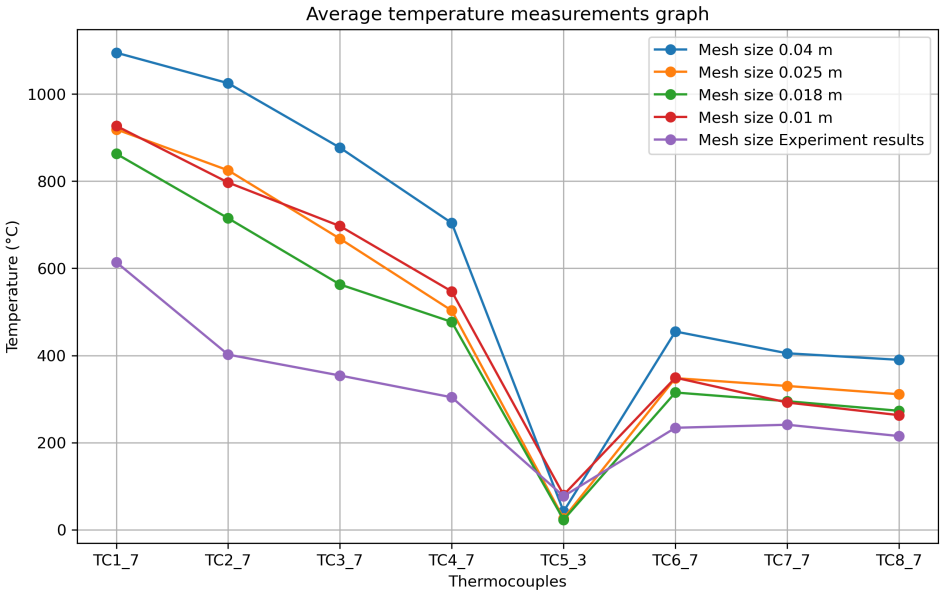

Figure 3.3: Graph of average temperatures illustrating the trend

4

Discussion

This chapter presents the main findings of this study and examines how this relates to the existing body of literature. It provides a summary of the research methodology and discusses the key modelling lessons derived from the project. Furthermore, it highlights the strengths and limitations of the study. The aim is to offer a comprehensive understanding of the research findings and laying the groundwork for subsequent conclusions and recommendations.

The study started with a literature review, which consisted both of full-scale and reduced-scale fire tests, as well as tutorials on how to conduct FDS simulations. When conducting the simulations, the modelling conditions have been adjusted with subsequent simulations to better reflect the real-life conditions and improve convergence with the experimental measurements. During the course of the simulations, four main simulations have been run with iterative refinement. The first three simulations involved progressively increasing the mesh resolution during the first three simulation, while the fourth simulation included adjustments to the material properties and application of multiple mesh boundaries to reduce the overall computation time.

4.1. Key Findings and Interpretation

The primary finding of this study is that, through the reproduction of the reduced-scale fire experiment using FDS simulations, the experimental measurements can be closely approximated. While this convergence does not occur in terms of raw numerical values, it does occur in terms of phenomenological similarities and trends. It is important to emphasis, that this outcome was anticipated at the beginning of the project. The fact is that fire experiments inherently involve highly complex phenomena, making their exact replication by means of simulations virtually impossible. Nevertheless, the ability to reproduce key trends and behaviours provide valuable insights, both in terms of the reliability of the simulations and future predictions. It is essential to note that the overall aim still is to improve FDS models further, such that they provide more reliable an accurate simulations, thereby more than only general trends in behaviour. The approximation of the simulation temperature results with experimental measurements can be interpreted in several ways. Firstly, the improvement in mesh resolution is a strong factor contributing to this outcome, as this contributes to the collection of more accurate results. Secondly, is refinement in various material properties, which has played a role. Although the effect is not as significant as the mesh size effect, it cannot be neglected. The adjustments in material properties include mainly the change of walls, ceiling and floor properties. For the previous simulations, these properties were set to the default *inert* setting. However, with the fourth simulation, the properties were adjusted to better reflect the experimental settings. As a result of this adjustments the heat reflection between the compartment space and the surrounding walls more closely matched the experiment conditions. In addition, the fuel release method were adjusted from heat release rate per unit area (HRRPUA) to mass flow rate, a method that more closely resembled the experiment conditions. It is difficult to determine to what degree these refinements led to the betterment of the simulation results, partly due to the limited number of simulations conducted. The reason for this limitation is the computationally demanding nature of the simulations, which require substantial precessing time to complete.

4.2. Connection to Existing Literature

In light of the existing literature and the rationale for the study, the implications of the study's findings for the literature the will be discussed. Conducting full-scale or even reduced-scale experiments in this region remains highly costly and difficult to do. Hence, drawing insights from FDS simulations to address gaps in the literature on fire spread in open-plan compartment would be highly important and beneficial. The findings of this study shows that drawing insights from FDS simulation is feasible and has a high value-to-cost ratio. The simulations that has been run during this study, although regrettably not many, still demonstrates noticeable improvements in replicating the experimental results. This suggests that with greater investment of resources in this area, it would be possible to achieve even more accurate reproductions of real-life fire experiments in open-plan compartments. Consequently, a broader range of scenarios would be explored through simulations, rather than physical fire experiment, thereby reducing the resources required to acquire valuable knowledge. Nevertheless, it must be acknowledged that a limited number of simulations has been conducted, due to the time-consuming nature of the simulations and the relatively short duration of the study. Consequently, it must be emphasised that such simulations are not without costs. The feasibility of FDS simulations require a substantial amount of computational power in order to maintain a practical runtime.

4.3. Modelling Lessons

There are several lessons that come to mind regarding the modelling of the simulations. First is the demanding nature of the simulations. The lack of computational resources would inevitable result in fewer amounts of simulations, thereby increasing the uncertainty associated with the observations. A more practical approach would involve reducing the simulation runtime by utilising greater computational power and refining the simulations through iterative modelling. Thereby, the reliance on assumptions would be reduced when it comes to interpreting the results of the simulations. Another important consideration is that simulations can never perfectly replicate real-life conditions. This is particularly true for complex phenomena such as fire spread. Even if models were able to perfectly reproduce the experimental setup, the experimental data inherently contain variability and noise that cannot be replicated in the simulations. For this reason, deviation from experiment results, even in relatively large amounts, should not be immediately interpreted as inaccuracies in the simulation outcomes.

4.4. Strengths and Limitations

The key strength of the results in this study is the consistent improvement observed across successive simulations. These iterative enhancements indicate that refining these simulation models is both feasible and practical, which also suggests that further refinements could increase the reliability of the models even more. The important limitation of this study is that, although the simulations outcomes demonstrate consistent improvements, the relatively small number of simulations remains a concern. This is also an inherent limitation of using FDS simulations to replicate fire experiments. The computationally demanding nature of such complex models can quickly make this approach impractical.

5

Conclusion and Recommendation

The objective of this study was to develop Fire Dynamics Simulator (FDS) numerical models, that is informed and validated by fire spread experiments conducted in a reduced-scale open-plan compartment. Throughout the research, the focus was on evaluating how accurately simulation models can replicate real fire spread behaviour and, in doing so, assess their potential to predict fire propagation scenarios and address gaps in the existing literature.

Open-plan compartments are increasingly common in modern urban environments, yet current prediction models of fire spread in these spaces remain limited. Although full-scale fire tests provide valuable insights, they often are extremely costly and destructive. Reduced-scale experiments offer a practical alternative, however, they still involve considerable costs and challenges. In this context, validated numerical simulations represent a practical and cost-effective solution, providing robust support to research on fire behaviour in open-plan compartments and enhancing our ability to predict fire propagation in real-world scenarios.

The outcomes of the four main simulations conducted in this study demonstrate that, through systematic refinements, numerical simulations can approximate experimental results. Key improvements included obtaining grid-independence, aligning material properties and fuel release mechanisms with the experimental setup, and implementing broader software enhancements to improve model accuracy. It is essential to note that considerable discrepancies remain between the numerical and experimental results, which should not be overlooked. These differences are likely attributable to not only the choice of simulation parameters, but also to the inherent difference between numerical simulations and real-life conditions. However, it is expected that with further refinements of simulation parameters, these discrepancies can be further minimised.

Remaining discrepancies between the simulation and experimental results, highlights the need for further research in this area. The recommendation for the future studies is to investigate these simulation models over a longer time duration and with increased data points to enhance reliability. Additionally, examining the effect of fuel release mechanisms and material properties, such as thermal conductivity and density on the results can provide useful insights. Finally, ventilation conditions in the simulation models likely have room for improvements and can be subject to further research. Collectively, these points underscore the continuous effort required to establish a solid and reliable framework for predicting fire behaviour in open-plan compartments.

A

Source Code Example

Example code on how the data is processed. `listings. \lstinputlisting[language=<Python>]{< }.`

```python
data = pd.read_csv("400mm_90.4kW_180s-mesh0.04m.csv", sep=';', skiprows=[0], dtype=str,
    engine='python')
data = data.apply(lambda col: col.str.replace(r',(?=\s|$)', '', regex=True))

for col in data.columns:
    data[col] = pd.to_numeric(data[col], errors='coerce')

for col in data.select_dtypes(include=[np.number]).columns:
    if np.allclose(data[col].dropna(), data[col].dropna().astype(int)):
        data[col] = data[col].astype("Int64")
data = data.round(2)

plt.figure(figsize=(14, 10))
plt.subplot(2, 2, 1)
plt.plot(data['Time'].head(180), data['TC1_7'].head(180), label='TC1_6')
plt.grid()
plt.xlabel('time in (s)')
plt.ylabel('Temperature in (degrees C)')
plt.title(f'TC1_7, AT: {data['TC1_7'].mean().round(0)} \u00B0C')

plt.subplot(2, 2, 2)
plt.plot(data['Time'].head(180), data['TC2_7'].head(180), label='TC2_7')
plt.grid()
plt.xlabel('time in (s)')
plt.ylabel('Temperature in (degrees C)')
plt.title(f'TC2_7, AT: {data['TC2_7'].mean().round(0)} \u00B0C')

plt.subplot(2, 2, 3)
plt.plot(data['Time'].head(180), data['TC7_7'].head(180), label='TC7_7', color='purple')
plt.grid()
plt.xlabel('time in (s)')
plt.ylabel('Temperature in (degrees C)')
plt.title(f'TC7_7, AT: {data['TC7_7'].mean().round(0)} \u00B0C')

plt.subplot(2, 2, 4)
plt.plot(data['Time'].head(180), data['TC8_7'].head(180), label='TC8_7', color='purple')
plt.grid()
plt.xlabel('time in (s)')
plt.ylabel('Temperature in (degrees C)')
plt.title(f'TC8_7, AT: {data['TC8_7'].mean().round(0)} \u00B0C');

subset = data.loc[5:90]

print(f'Average temperature of TC1_6: {subset['TC1_7'].mean().round(0)}\u00B0C')
print(f'Average temperature of TC2_7: {subset['TC2_7'].mean().round(0)}\u00B0C')
print(f'Average temperature of TC3_7: {subset['TC3_7'].mean().round(0)}\u00B0C')
print(f'Average temperature of TC4_7: {subset['TC4_7'].mean().round(0)}\u00B0C')
```

```
47 print(f'Average␣temperature␣of␣TC5_7:␣{subset['TC5_7'].mean().round(0)}\u00B0C')
48 print(f'Average␣temperature␣of␣TC6_7:␣{subset['TC6_7'].mean().round(0)}\u00B0C')
49 print(f'Average␣temperature␣of␣TC7_7:␣{subset['TC7_7'].mean().round(0)}\u00B0C')
50 print(f'Average␣temperature␣of␣TC8_7:␣{subset['TC8_7'].mean().round(0)}\u00B0C')
51 print(f'Average␣temperature␣of␣TC5_3:␣{subset['TC5_3'].mean().round(0)}\u00B0C')
```

B

Planning

Here comes the tasks and deadlines.

Table B.1: Distribution of the workload

	Task	Deadline(s)
	Summary	31-10-2025
Chapter 1	Introduction	13-09-2025
Chapter 2	Empirical Experminent and Data	27-09-2025
Chapter 3	FDS Simulation	27-09-2025
Chapter 4	Results and Discussion	27-10-2025
Chapter 5	Conclusion	30-10-2025
	Editors	31-10-2025
	Figures	31-10-2025
	Document Design and Layout	31-10-2025

C

References

Sources

author = Rainbow-Restoration, title = Rainbow-Restoration, year = 2025,
url = https://rainbowrestores.com/blog/house-fire-statistics#:~:text=The%20leading%20cause%20of%20house,of%20all%20fire%2Drelated%20injuries., urldate = 2025-09-09,

author = Wikipedia, title = Grenfell Tower Fire, url = https://en.wikipedia.org/wiki/Grenfell_Tower_fire urldate = 2025-09-13, year = 2025,

author = Wikipedia, title = The fire during the early morning hours of 14 June 2017, year = 2025, url = https://en.wikipedia.org/wiki/File:Grenfell_Tower_fire_(wider_view).jpg, urldate = 2025-09-13,

author = Wallpaper.com, title = Sunset Wallpapers, year = 2025, url = https://wallpapers.com/sunset , urldate = 2025-09-13,

authors = Xu Dai, Antonio Gamba, Stephen Welch, Chang Liu , Johan Anderson, Marion Charlier, David Rush, Stephen Welch , title = An engineering CFD model for fire spread on wood cribs for travelling fires, year = 2022,
url = https://www.sciencedirect.com/science/article/pii /S0965997822001181 , urldate = 2025-09-20,

authors = Zhuojun Nan, Aatif Ali Khan, Liming Jiang, Suwen Chen, Asif Usmani , title = Application of travelling behaviour models for thermal responses in large compartment fires, year = 2022,
url = https://www.sciencedirect.com/science/article/pii/ S0379711222001795 , urldate = 2025-09-20,

authors = Jamie Stern-Gottfried, Guillermo Rein, title = Travelling fires for structural design–Part I: Literature review, year = 2012, url = https://doi.org/10.1016/j.firesaf.2012.06.003 , urldate = 2025-09-21,

authors = Sam Nothard, David Lange, Juan P. Hidalgo, Vinny Gupta, Martyn S. McLaggan, Felix Wiesner, Jose L. Torero, title = Factors influencing the fire dynamics in open-plan compartments with an exposed timber ceiling, year = 2022, url = https://www.sciencedirect.com/science/article/pii/S037971122200042X , urldate = 2025-09-22,

authors = Andrea, title = FDS Mesh size calculator, year = 2021, url = https://fdstutorial.com/fds-mesh-size-calculator/ , urldate = 2025-10-19,

authors = Ricardo Gasparini, title = Mesh Sensitivity Study for CDF Simulations, year = 2022, url = https://www.simscale.com/knowledge-base/mesh-sensitivity-cfd/ , urldate = 2025-10-29,

authors = Thunderhead Engineering, title = PyroSim User Manual, year = 2025,
url = https://support.thunderheadeng.com/docs/pyrosim/2025-1/user-manual/ ,

authors = Kevin B. McGrattan, Glenn P. Forney, Jason E. Floyd, Simo Hostikka , title = Fire Dynamics Simulator (Version 2)– User's Guide, year = 2001,
url = https://nvlpubs.nist.gov/nistpubs/Legacy/IR/nistir6784.pdf , urldate = 2025-10-29,

D

Average temperature table

	90.4 kW	60.3 kW	45.2 kW	37.7 kW	30.1 kW	22.6 kW
TC1_1	370.7836	290.4435	270.3431	221.2697	169.6041	123.7649
TC1_2	393.7720	292.4839	277.0573	228.4283	174.8833	124.4590
TC1_3	422.3585	286.0039	268.1415	220.2692	168.3352	117.7971
TC1_4	488.1618	319.2177	283.6307	236.5122	182.1853	127.8720
TC1_5	575.1694	391.2649	336.0640	291.3481	233.1783	172.4148
TC1_6	614.3639	455.7671	400.9121	360.9816	304.4787	233.4552
TC1_7	624.5111	488.4223	436.5029	400.0512	345.1158	268.1541
TC2_1	147.2730	114.4582	88.1989	78.0182	67.7091	56.5749
TC2_2	159.8592	121.6954	96.2365	83.9925	71.9180	58.8373
TC2_3	166.8973	120.6146	97.5821	85.4177	73.9274	61.0854
TC2_4	276.2335	187.4488	144.4508	127.0170	107.3913	91.3028
TC2_5	411.9003	276.9973	219.8801	194.3653	167.4613	138.8473
TC2_6	437.3271	316.9027	265.7643	238.1383	207.3818	169.1624
TC2_7	401.6835	309.7863	265.9104	240.6075	211.5176	173.8714
TC3_1	112.5904	88.9746	72.1799	64.4899	56.5861	48.7377
TC3_2	120.1072	93.5265	76.4019	68.1625	59.4167	50.3430
TC3_3	121.6887	91.8765	75.6687	66.7302	59.1853	49.3528
TC3_4	228.5472	163.5560	128.9552	112.5298	96.0069	80.3604
TC3_5	328.5382	235.1847	194.8915	177.0237	154.2949	130.0624
TC3_6	365.6260	265.1101	222.6655	203.6748	179.6316	149.1858
TC3_7	353.7405	267.8240	230.9956	211.7932	187.5566	155.3359
TC4_1	80.9729	65.5558	57.1461	51.8882	47.1458	41.7585
TC4_2	89.5977	73.0626	61.8665	56.2428	50.6498	44.0662
TC4_3	89.2295	72.2544	61.1725	55.3069	50.2476	43.3728
TC4_4	153.9346	119.9225	89.1777	75.8122	66.6071	56.7802
TC4_5	263.1700	200.4599	173.4094	157.1814	137.7798	116.4136
TC4_6	303.5622	232.3865	206.3428	191.0107	169.9432	142.7673
TC4_7	323.7064	250.0450	223.8746	208.2758	186.0370	155.1253
TC5_1	72.4259	60.6196	53.8098	49.3390	44.7590	40.1879
TC5_2	72.5561	60.0170	53.2047	49.0721	44.9449	39.8687
TC5_3	77.2237	66.2129	56.1974	51.4202	47.6817	42.7356
TC6_7	233.8299	196.0698	181.3990	168.4464	151.5383	127.3915
TC7_1	54.8470	47.9402	44.2251	41.5931	38.9414	35.5000
TC7_2	58.7603	50.2958	46.7144	43.7055	40.7711	36.9477
TC7_3	79.8172	67.1502	54.2701	49.2856	44.5289	39.4230
TC7_4	140.3338	118.0216	101.6541	92.4840	80.6375	70.1194
TC7_5	186.8136	153.6721	136.7999	126.3541	113.7667	98.9540
TC7_6	228.2844	185.8259	168.9305	155.1828	139.4841	119.1057
TC7_7	240.9905	197.6802	182.3901	168.5122	152.2903	129.1733
TC8_1	53.9419	47.8952	44.4603	41.7412	39.1757	35.9977
TC8_2	55.3022	48.9728	45.4399	42.5614	39.9716	36.5935
TC8_3	84.6631	66.1338	52.5640	47.3222	43.1594	38.8019
TC8_4	167.1120	134.9553	114.9029	102.8130	89.6090	74.1887
TC8_5	191.4861	158.4480	143.3606	133.1924	121.0272	104.4706
TC8_6	205.3170	171.4759	156.5113	145.0637	131.8538	113.1381
TC8_7	215.5204	181.8954	167.8999	155.9033	141.6879	121.1498

Table D.1: Table of measured temperatures (in degrees Celcius) across different HRR's(Dr. Zhuojun Nan).

E

Table of Simulation Temperature Results

Mesh size	0.01 m	0.018 m	0.025 m	0.04 m	Experiment results
TC1_1	330.5398	25.9552	23.5164	26.9518	370.7836
TC1_2	376.7843	29.2056	26.1136	52.2781	393.7720
TC1_3	426.8633	38.4782	54.5082	91.5046	422.3585
TC1_4	545.5594	109.6408	214.1629	168.0638	488.1618
TC1_5	767.7299	401.5736	565.9242	362.7824	575.1694
TC1_6	841.3618	807.6982	909.4777	1067.0191	614.3639
TC1_7	N/A	N/A	N/A	N/A	624.5111
TC2_1	203.3172	24.6474	23.1850	25.1158	147.2730
TC2_2	222.8365	25.6289	23.1209	34.2079	159.8592
TC2_3	238.1534	26.9844	29.5953	49.8654	166.8973
TC2_4	358.5885	44.5639	108.5565	104.3743	276.2335
TC2_5	634.8230	283.6543	439.2828	278.0414	411.9003
TC2_6	708.1572	675.4051	823.8956	994.5697	437.3271
TC2_7	762.4345	675.4051	823.8956	994.5697	401.6835
TC3_1	134.3718	23.7754	22.5618	24.2677	112.5904
TC3_2	147.5621	24.7685	23.2631	31.1023	120.1072
TC3_3	162.2223	25.9244	31.2720	45.4693 7	121.6887
TC3_4	291.0115	209.9390	286.3330	215.5821	228.5472
TC3_5	516.2418	40.5698	76.1974	93.4351	328.5382
TC3_6	591.8787	549.1000	662.2168	850.4233	365.6260
TC3_7	662.7358	549.1000	662.2168	850.4233	353.7405
TC4_1	87.5062	22.3834	22.1818	24.0838	80.9729
TC4_2	96.5880	23.6189	22.9158	30.2844	89.5977
TC4_3	106.2806	25.3056	26.1616	41.0076	89.2295
TC4_4	260.1225	160.8469	197.6515	167.4893	153.9346
TC4_5	394.8939	37.7200	55.7221	76.3591	263.1700
TC4_6	454.8442	442.8918	502.5429	682.4837	303.5622
TC4_7	519.8309	442.8918	502.5429	682.4837	323.7064
TC5_1	59.9889	21.3813	21.6769	23.9300	72.4259
TC5_2	65.3630	21.8925	22.1485	29.9976	72.5561
TC5_3	73.9714	23.6769	25.7040	40.9523	77.2237
TC5_4	196.0669	150.9015	172.2888	149.4411	N/A
TC5_5	308.8544	34.8315	52.9477	72.1012	N/A
TC5_6	356.3312	340.9662	397.9576	516.4585	N/A
TC5_7	409.5648	340.9662	397.9576	516.4585	N/A
TC6_1	46.8488	21.0590	21.4224	23.0962	N/A
TC6_2	52.2474	21.4805	21.8310	30.3711	N/A
TC6_3	64.0965	24.2956	26.3579	43.3568	N/A
TC6_4	160.9497	156.9010	187.6964	151.8852	N/A
TC6_5	250.5043	45.3334	65.4541	77.5847	N/A
TC6_6	289.1424	298.1926	342.1736	438.5952	N/A
TC6_7	333.0952	298.1926	342.1736	438.5952	233.8299
TC7_1	38.7996	20.8285	20.9563	22.3126	54.8470
TC7_2	46.9670	22.2682	21.8416	32.3056	58.7603
TC7_3	70.9621	28.6202	31.8325	49.6081	79.8172
TC7_4	163.4629	185.6302	223.1320	180.0344	140.3338
TC7_5	219.8866	79.0697	92.6783	93.1478	186.8136
TC7_6	245.7599	280.4451	325.0735	389.7785	228.2844
TC7_7	275.9387	280.4451	325.0735	389.7785	240.9905
TC8_1	36.6881	22.6682	24.7776	24.5207	53.9419
TC8_2	52.1535	26.0957	28.2026	41.5496	55.3022
TC8_3	89.6047	45.5474	48.3421	63.6400	84.6631
TC8_4	187.4409	221.1893	246.1227	214.0684	167.1120
TC8_5	220.5334	118.5082	118.2403	113.1933	191.4861
TC8_6	233.1482	268.5792	315.4489	374.5880	205.3170
TC8_7	247.2167	268.5792	315.4489	374.5880	215.5204

Table E.1: Average temperature comparison for different mesh sizes.

F

Temperature Results Visualisation

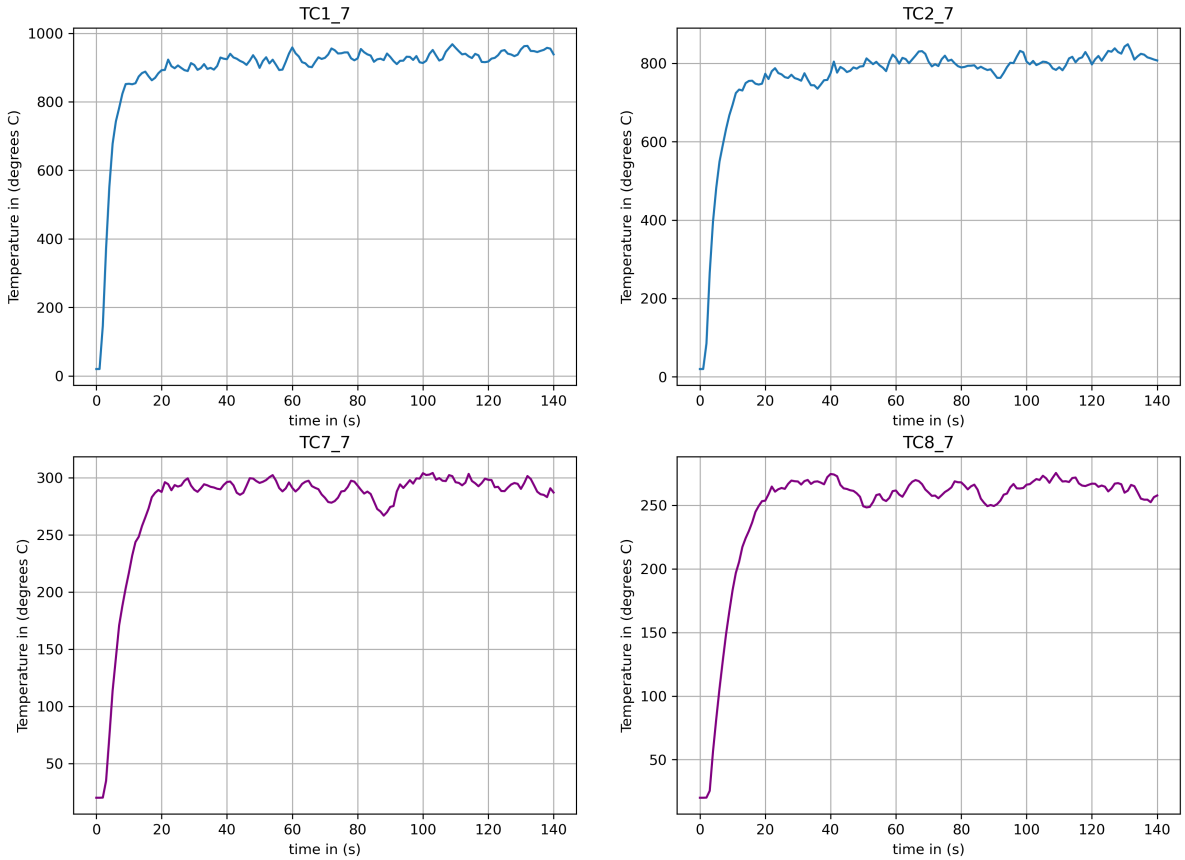

Figure F.1: Temperature measurements of different thermocouples from simulation with mesh size 0.01 m.

G

FDS File

```
&HEAD CHID='Line_Burner_0mm', TITLE='Test a liner burner in a reduced scale compartment with no edge beam'/

TIME T_END=0.0 / Test model set-up
&TIME T_END=6900.0 / Run
&DUMP DT_RESTART = 10, NFRAMES = 3450, DT_DEVC=1., DT_HRR=1., SIG_FIGS=4, SIG_FIGS_EXP=2 / Define how often outputs are saved, DT_RESTART should be used for simulations running on supercomputers

MISC RESTART = .TRUE., TMPA = 20. / change this to .TRUE. for restart run
&MISC RESTART = .FALSE., TMPA = 20. /

&RADI NUMBER_RADIATION_ANGLES=400 /

********************************* Fire Zone *********************************
    0.01 m cube
&MESH ID = 'Mesh_01', IJK =  42, 40, 14, XB = -0.80, -0.38, 0.00, 0.40, -0.04, 0.10, COLOR='RAINBOW', MPI_PROCESS=0  / 23,520 cells
&MESH ID = 'Mesh_02', IJK =  42, 40, 14, XB = -0.80, -0.38, 0.40, 0.80, -0.04, 0.10, COLOR='RAINBOW', MPI_PROCESS=1  / 23,520 cells
&MESH ID = 'Mesh_03', IJK =  42, 40, 14, XB = -0.38,  0.04, 0.00, 0.40, -0.04, 0.10, COLOR='RAINBOW', MPI_PROCESS=2  / 23,520 cells
&MESH ID = 'Mesh_04', IJK =  42, 40, 14, XB = -0.38,  0.04, 0.40, 0.80, -0.04, 0.10, COLOR='RAINBOW', MPI_PROCESS=3  / 23,520 cells
&MESH ID = 'Mesh_05', IJK =  42, 40, 10, XB = -0.80, -0.38, 0.00, 0.40,  0.10, 0.20, COLOR='RAINBOW', MPI_PROCESS=4  / 16,800 cells
&MESH ID = 'Mesh_06', IJK =  42, 40, 10, XB = -0.80, -0.38, 0.40, 0.80,  0.10, 0.20, COLOR='RAINBOW', MPI_PROCESS=5  / 16,800 cells
&MESH ID = 'Mesh_07', IJK =  42, 40, 10, XB = -0.38,  0.04, 0.00, 0.40,  0.10, 0.20, COLOR='RAINBOW', MPI_PROCESS=6  / 16,800 cells
&MESH ID = 'Mesh_08', IJK =  42, 40, 10, XB = -0.38,  0.04, 0.40, 0.80,  0.10, 0.20, COLOR='RAINBOW', MPI_PROCESS=7  / 16,800 cells
&MESH ID = 'Mesh_09', IJK =  42, 40, 10, XB = -0.80, -0.38, 0.00, 0.40,  0.20, 0.30, COLOR='RAINBOW', MPI_PROCESS=8  / 16,800 cells
&MESH ID = 'Mesh_10', IJK =  42, 40, 10, XB = -0.80, -0.38, 0.40, 0.80,  0.20, 0.30, COLOR='RAINBOW', MPI_PROCESS=9  / 16,800 cells
&MESH ID = 'Mesh_11', IJK =  42, 40, 10, XB = -0.38,  0.04, 0.00, 0.40,  0.20, 0.30, COLOR='RAINBOW', MPI_PROCESS=10 / 16,800 cells
&MESH ID = 'Mesh_12', IJK =  42, 40, 10, XB = -0.38,  0.04, 0.40, 0.80,  0.20, 0.30, COLOR='RAINBOW', MPI_PROCESS=11 / 16,800 cells
&MESH ID = 'Mesh_13', IJK =  42, 40, 12, XB = -0.80, -0.38, 0.00, 0.40,  0.30, 0.42, COLOR='RAINBOW', MPI_PROCESS=12 / 20,160 cells
```

```
&MESH ID = 'Mesh_14', IJK =  42, 40, 12, XB = -0.80, -0.38, 0.40, 0.80,  0.30,
    0.42, COLOR='RAINBOW', MPI_PROCESS=13 / 20,160 cells
&MESH ID = 'Mesh_15', IJK =  42, 40, 12, XB = -0.38,  0.04, 0.00, 0.40,  0.30,
    0.42, COLOR='RAINBOW', MPI_PROCESS=14 / 20,160 cells
&MESH ID = 'Mesh_16', IJK =  42, 40, 12, XB = -0.38,  0.04, 0.40, 0.80,  0.30,
    0.42, COLOR='RAINBOW', MPI_PROCESS=15 / 20,160 cells
********************************************************************************

************************** Inside Compartment ******************************
    0.02 m cube
&MESH ID = 'Mesh_17', IJK =  38, 20, 23, XB = -2.32, -1.56, 0.00, 0.40, -0.04,
    0.42, COLOR='RAINBOW', MPI_PROCESS=16 / 17,480 cells
&MESH ID = 'Mesh_18', IJK =  38, 20, 23, XB = -2.32, -1.56, 0.40, 0.80, -0.04,
    0.42, COLOR='RAINBOW', MPI_PROCESS=17 / 17,480 cells
&MESH ID = 'Mesh_19', IJK =  38, 20, 23, XB = -1.56, -0.80, 0.00, 0.40, -0.04,
    0.42, COLOR='RAINBOW', MPI_PROCESS=18 / 17,480 cells
&MESH ID = 'Mesh_20', IJK =  38, 20, 23, XB = -1.56, -0.80, 0.40, 0.80, -0.04,
    0.42, COLOR='RAINBOW', MPI_PROCESS=19 / 17,480 cells
********************************************************************************

************************ Outside Compartment (Front) ************************
    0.02 m cube
&MESH ID = 'Mesh_21', IJK =  38, 20, 33, XB = -2.32, -1.56,-0.40, 0.00, -0.04,
    0.62, COLOR='RAINBOW', MPI_PROCESS=20 / 25,080 cells
&MESH ID = 'Mesh_22', IJK =  38, 20, 33, XB = -1.56, -0.80,-0.40, 0.00, -0.04,
    0.62, COLOR='RAINBOW', MPI_PROCESS=21 / 25,080 cells
&MESH ID = 'Mesh_23', IJK =  42, 20, 33, XB = -0.80,  0.04,-0.40, 0.00, -0.04,
    0.62, COLOR='RAINBOW', MPI_PROCESS=22 / 25,080 cells
********************************************************************************

************************ Outside Compartment (Above) ************************
    0.02 m cube
&MESH ID = 'Mesh_24', IJK =  38, 40, 10, XB = -2.32, -1.56, 0.00, 0.80,  0.42,
    0.62, COLOR='RAINBOW', MPI_PROCESS=23 / 15,200 cells
&MESH ID = 'Mesh_25', IJK =  38, 40, 10, XB = -1.56, -0.80, 0.00, 0.80,  0.42,
    0.62, COLOR='RAINBOW', MPI_PROCESS=24 / 15,200 cells
&MESH ID = 'Mesh_26', IJK =  42, 40, 10, XB = -0.80,  0.04, 0.00, 0.80,  0.42,
    0.62, COLOR='RAINBOW', MPI_PROCESS=25 / 16,800 cells
********************************************************************************

&VENT MB='ZMIN',SURF_ID='OPEN'/
&VENT MB='ZMAX',SURF_ID='OPEN'/
&VENT MB='YMIN',SURF_ID='OPEN'/
&VENT MB='YMAX',SURF_ID='OPEN'/
&VENT MB='XMIN',SURF_ID='OPEN'/
&VENT MB='XMAX',SURF_ID='OPEN'/ Define domain boundaries


&REAC ID='PROPANE_BURNING',
      FUEL='PROPANE',
      CO_YIELD=0.005,
      SOOT_YIELD=0.01,
      RADIATIVE_FRACTION=0.35
      HEAT_OF_COMBUSTION=46450.  / yCO, ySoot from Table A.39, p.3466 & Table A
          .40, p.3472 in SFPE, HoC from Table 1.13, p.21 in Drysdale

&SURF ID='Line_Burner', MASS_FLUX(1)=0.0772, SPEC_ID(1)='PROPANE', RAMP_MF(1)='
    PROPANE_FLOW_RAMP', COLOR='RED' / Assume propane density 1.833 kg m-3 at 20 C,
    MASS FLUX unit in kg m-2 s-1
&RAMP ID='PROPANE_FLOW_RAMP', T= 0., F=0.0 /
&RAMP ID='PROPANE_FLOW_RAMP', T= 1., F=1.0 /
```

```
&RAMP ID='PROPANE_FLOW_RAMP', T=900., F=1.0 /
&RAMP ID='PROPANE_FLOW_RAMP', T=901., F=0.667 /
&RAMP ID='PROPANE_FLOW_RAMP', T=1800., F=0.667 /
&RAMP ID='PROPANE_FLOW_RAMP', T=1801., F=0.417 /
&RAMP ID='PROPANE_FLOW_RAMP', T=2700., F=0.417 /
&RAMP ID='PROPANE_FLOW_RAMP', T=2701., F=0.333 /
&RAMP ID='PROPANE_FLOW_RAMP', T=3600., F=0.333 /
&RAMP ID='PROPANE_FLOW_RAMP', T=3601., F=0.250 /
&RAMP ID='PROPANE_FLOW_RAMP', T=4500., F=0.250 /

&VENT ID='Vent', SURF_ID='Line_Burner', XB = -0.22, -0.17, 0.15, 0.625, 0.00, 0.00 /

&MATL ID='VERMICULITE',
      SPECIFIC_HEAT=0.94,
      CONDUCTIVITY=0.12,
      DENSITY=375.0,
      EMISSIVITY=0.9 / Reported in Nothard et al. 2022 FSJ

&MATL ID='PLASTERBOARD',
      SPECIFIC_HEAT=1.09,
      CONDUCTIVITY=0.24,
      DENSITY=780.0,
      EMISSIVITY=0.89 / Reported in Nothard et al. 2022 FSJ

&MATL ID='CERAMIC_WOOL',
      SPECIFIC_HEAT=1.13,
      CONDUCTIVITY=0.09,
      DENSITY=96.0,
      EMISSIVITY=0.9 / Reported in Nothard et al. 2022 FSJ

&SURF ID                    = 'CEILING_TOP_TO_BOTTOM'
          MATL_ID           = 'PLASTERBOARD', 'CERAMIC_WOOL'
          RGB           = 225,206,167
          THICKNESS         = 0.016, 0.005
          TRANSPARENCY  = 1.0 /

&SURF ID                    = 'CEILING_BOTTOM_TO_TOP'
          MATL_ID           = 'CERAMIC_WOOL', 'PLASTERBOARD'
          RGB           = 225,206,167
          THICKNESS         = 0.005, 0.016
          TRANSPARENCY  = 1.0 /

&SURF ID   = 'UNEXPOSED'
      RGB  = 225,206,167  / i.e. inert by default


&SURF ID = 'FLOOR', MATL_ID = 'VERMICULITE', THICKNESS = 0.04, TRANSPARENCY = 1.0, RGB = 225,206,167 /
&SURF ID = 'WALLS', MATL_ID = 'VERMICULITE', THICKNESS = 0.04, TRANSPARENCY = 1.0, RGB = 225,206,167/


&OBST ID = 'Floor',     XB = -2.24, -0.04, 0.00, 0.76, -0.04, 0.00, SURF_ID='FLOOR' /
&OBST ID = 'Left_wall', XB = -2.28, -2.24, 0.00, 0.80, -0.04, 0.40, SURF_ID='WALLS' /
&OBST ID = 'Rear_wall', XB = -2.24, -0.04, 0.76, 0.80, -0.04, 0.40, SURF_ID='WALLS' /
&OBST ID = 'Right_wall',XB = -0.04,  0.00, 0.00, 0.80, -0.04, 0.40, SURF_ID='WALLS' /
```

```
122 &OBST ID = 'Ceiling',   XB = -2.28,  0.00, 0.00, 0.80,  0.40, 0.42, SURF_ID6 = '
    UNEXPOSED','UNEXPOSED','UNEXPOSED','UNEXPOSED','CEILING_BOTTOM_TO_TOP','
    CEILING_TOP_TO_BOTTOM' /
123
124
125 &PROP ID='TC_props', DIAMETER=1.5E-3, EMISSIVITY=0.9/
126 &DEVC ID='TC8_1', PROP_ID='TC_props', QUANTITY='THERMOCOUPLE', XYZ=-2.015,0.4,0.13
      /
127 &DEVC ID='TC8_2', PROP_ID='TC_props', QUANTITY='THERMOCOUPLE', XYZ=-2.015,0.4,0.18
      /
128 &DEVC ID='TC8_3', PROP_ID='TC_props', QUANTITY='THERMOCOUPLE', XYZ=-2.015,0.4,0.23
      /
129 &DEVC ID='TC8_4', PROP_ID='TC_props', QUANTITY='THERMOCOUPLE', XYZ=-2.015,0.4,0.28
      /
130 &DEVC ID='TC8_5', PROP_ID='TC_props', QUANTITY='THERMOCOUPLE', XYZ=-2.015,0.4,0.33
      /
131 &DEVC ID='TC8_6', PROP_ID='TC_props', QUANTITY='THERMOCOUPLE', XYZ
    =-2.015,0.4,0.355/
132 &DEVC ID='TC8_7', PROP_ID='TC_props', QUANTITY='THERMOCOUPLE', XYZ=-2.015,0.4,0.37
      /
133
134 &DEVC ID='TC7_1', PROP_ID='TC_props', QUANTITY='THERMOCOUPLE', XYZ=-1.765,0.4,0.13
      /
135 &DEVC ID='TC7_2', PROP_ID='TC_props', QUANTITY='THERMOCOUPLE', XYZ=-1.765,0.4,0.18
      /
136 &DEVC ID='TC7_3', PROP_ID='TC_props', QUANTITY='THERMOCOUPLE', XYZ=-1.765,0.4,0.23
      /
137 &DEVC ID='TC7_4', PROP_ID='TC_props', QUANTITY='THERMOCOUPLE', XYZ=-1.765,0.4,0.28
      /
138 &DEVC ID='TC7_5', PROP_ID='TC_props', QUANTITY='THERMOCOUPLE', XYZ=-1.765,0.4,0.33
      /
139 &DEVC ID='TC7_6', PROP_ID='TC_props', QUANTITY='THERMOCOUPLE', XYZ
    =-1.765,0.4,0.355/
140 &DEVC ID='TC7_7', PROP_ID='TC_props', QUANTITY='THERMOCOUPLE', XYZ=-1.765,0.4,0.37
      /
141
142 &DEVC ID='TC6_1', PROP_ID='TC_props', QUANTITY='THERMOCOUPLE', XYZ=-1.515,0.4,0.13
      /
143 &DEVC ID='TC6_2', PROP_ID='TC_props', QUANTITY='THERMOCOUPLE', XYZ=-1.515,0.4,0.18
      /
144 &DEVC ID='TC6_3', PROP_ID='TC_props', QUANTITY='THERMOCOUPLE', XYZ=-1.515,0.4,0.23
      /
145 &DEVC ID='TC6_4', PROP_ID='TC_props', QUANTITY='THERMOCOUPLE', XYZ=-1.515,0.4,0.28
      /
146 &DEVC ID='TC6_5', PROP_ID='TC_props', QUANTITY='THERMOCOUPLE', XYZ=-1.515,0.4,0.33
      /
147 &DEVC ID='TC6_6', PROP_ID='TC_props', QUANTITY='THERMOCOUPLE', XYZ
    =-1.515,0.4,0.355/
148 &DEVC ID='TC6_7', PROP_ID='TC_props', QUANTITY='THERMOCOUPLE', XYZ=-1.515,0.4,0.37
      /
149
150 &DEVC ID='TC5_1', PROP_ID='TC_props', QUANTITY='THERMOCOUPLE', XYZ=-1.265,0.4,0.13
      /
151 &DEVC ID='TC5_2', PROP_ID='TC_props', QUANTITY='THERMOCOUPLE', XYZ=-1.265,0.4,0.18
      /
152 &DEVC ID='TC5_3', PROP_ID='TC_props', QUANTITY='THERMOCOUPLE', XYZ=-1.265,0.4,0.23
      /
153 &DEVC ID='TC5_4', PROP_ID='TC_props', QUANTITY='THERMOCOUPLE', XYZ=-1.265,0.4,0.28
      /
154 &DEVC ID='TC5_5', PROP_ID='TC_props', QUANTITY='THERMOCOUPLE', XYZ=-1.265,0.4,0.33
      /
```

```
155 &DEVC ID='TC5_6', PROP_ID='TC_props', QUANTITY='THERMOCOUPLE', XYZ
    =-1.265,0.4,0.355/
156 &DEVC ID='TC5_7', PROP_ID='TC_props', QUANTITY='THERMOCOUPLE', XYZ=-1.265,0.4,0.37
     /
157
158 &DEVC ID='TC4_1', PROP_ID='TC_props', QUANTITY='THERMOCOUPLE', XYZ=-1.015,0.4,0.13
     /
159 &DEVC ID='TC4_2', PROP_ID='TC_props', QUANTITY='THERMOCOUPLE', XYZ=-1.015,0.4,0.18
     /
160 &DEVC ID='TC4_3', PROP_ID='TC_props', QUANTITY='THERMOCOUPLE', XYZ=-1.015,0.4,0.23
     /
161 &DEVC ID='TC4_4', PROP_ID='TC_props', QUANTITY='THERMOCOUPLE', XYZ=-1.015,0.4,0.28
     /
162 &DEVC ID='TC4_5', PROP_ID='TC_props', QUANTITY='THERMOCOUPLE', XYZ=-1.015,0.4,0.33
     /
163 &DEVC ID='TC4_6', PROP_ID='TC_props', QUANTITY='THERMOCOUPLE', XYZ
    =-1.015,0.4,0.355/
164 &DEVC ID='TC4_7', PROP_ID='TC_props', QUANTITY='THERMOCOUPLE', XYZ=-1.015,0.4,0.37
     /
165
166 &DEVC ID='TC3_1', PROP_ID='TC_props', QUANTITY='THERMOCOUPLE', XYZ=-0.765,0.4,0.13
     /
167 &DEVC ID='TC3_2', PROP_ID='TC_props', QUANTITY='THERMOCOUPLE', XYZ=-0.765,0.4,0.18
     /
168 &DEVC ID='TC3_3', PROP_ID='TC_props', QUANTITY='THERMOCOUPLE', XYZ=-0.765,0.4,0.23
     /
169 &DEVC ID='TC3_4', PROP_ID='TC_props', QUANTITY='THERMOCOUPLE', XYZ=-0.765,0.4,0.28
     /
170 &DEVC ID='TC3_5', PROP_ID='TC_props', QUANTITY='THERMOCOUPLE', XYZ=-0.765,0.4,0.33
     /
171 &DEVC ID='TC3_6', PROP_ID='TC_props', QUANTITY='THERMOCOUPLE', XYZ
    =-0.765,0.4,0.355/
172 &DEVC ID='TC3_7', PROP_ID='TC_props', QUANTITY='THERMOCOUPLE', XYZ=-0.765,0.4,0.37
     /
173
174 &DEVC ID='TC2_1', PROP_ID='TC_props', QUANTITY='THERMOCOUPLE', XYZ=-0.515,0.4,0.13
     /
175 &DEVC ID='TC2_2', PROP_ID='TC_props', QUANTITY='THERMOCOUPLE', XYZ=-0.515,0.4,0.18
     /
176 &DEVC ID='TC2_3', PROP_ID='TC_props', QUANTITY='THERMOCOUPLE', XYZ=-0.515,0.4,0.23
     /
177 &DEVC ID='TC2_4', PROP_ID='TC_props', QUANTITY='THERMOCOUPLE', XYZ=-0.515,0.4,0.28
     /
178 &DEVC ID='TC2_5', PROP_ID='TC_props', QUANTITY='THERMOCOUPLE', XYZ=-0.515,0.4,0.33
     /
179 &DEVC ID='TC2_6', PROP_ID='TC_props', QUANTITY='THERMOCOUPLE', XYZ
    =-0.515,0.4,0.355/
180 &DEVC ID='TC2_7', PROP_ID='TC_props', QUANTITY='THERMOCOUPLE', XYZ=-0.515,0.4,0.37
     /
181
182 &DEVC ID='TC1_1', PROP_ID='TC_props', QUANTITY='THERMOCOUPLE', XYZ=-0.265,0.4,0.13
     /
183 &DEVC ID='TC1_2', PROP_ID='TC_props', QUANTITY='THERMOCOUPLE', XYZ=-0.265,0.4,0.18
     /
184 &DEVC ID='TC1_3', PROP_ID='TC_props', QUANTITY='THERMOCOUPLE', XYZ=-0.265,0.4,0.23
     /
185 &DEVC ID='TC1_4', PROP_ID='TC_props', QUANTITY='THERMOCOUPLE', XYZ=-0.265,0.4,0.28
     /
186 &DEVC ID='TC1_5', PROP_ID='TC_props', QUANTITY='THERMOCOUPLE', XYZ=-0.265,0.4,0.33
     /
```

```
&DEVC ID='TC1_6', PROP_ID='TC_props', QUANTITY='THERMOCOUPLE', XYZ
    =-0.265,0.4,0.355/
&DEVC ID='TC1_7', PROP_ID='TC_props', QUANTITY='THERMOCOUPLE', XYZ=-0.265,0.4,0.37
     /

&DEVC ID='TSC_C_1', QUANTITY='INCIDENT HEAT FLUX', XYZ=-0.265,0.4,0.4, IOR=-3/
&DEVC ID='TSC_C_2', QUANTITY='INCIDENT HEAT FLUX', XYZ=-0.515,0.4,0.4, IOR=-3/
&DEVC ID='TSC_C_3', QUANTITY='INCIDENT HEAT FLUX', XYZ=-0.765,0.4,0.4, IOR=-3/
&DEVC ID='TSC_C_4', QUANTITY='INCIDENT HEAT FLUX', XYZ=-1.015,0.4,0.4, IOR=-3/
&DEVC ID='TSC_C_5', QUANTITY='INCIDENT HEAT FLUX', XYZ=-1.265,0.4,0.4, IOR=-3/
&DEVC ID='TSC_C_6', QUANTITY='INCIDENT HEAT FLUX', XYZ=-1.515,0.4,0.4, IOR=-3/
&DEVC ID='TSC_C_7', QUANTITY='INCIDENT HEAT FLUX', XYZ=-1.765,0.4,0.4, IOR=-3/
&DEVC ID='TSC_C_8', QUANTITY='INCIDENT HEAT FLUX', XYZ=-2.015,0.4,0.4, IOR=-3/
&DEVC ID='TSC_F_01', QUANTITY='INCIDENT HEAT FLUX', XYZ=-0.265,0.4,0.0, IOR=3/
&DEVC ID='TSC_F_02', QUANTITY='INCIDENT HEAT FLUX', XYZ=-0.515,0.4,0.0, IOR=3/
&DEVC ID='TSC_F_03', QUANTITY='INCIDENT HEAT FLUX', XYZ=-0.765,0.4,0.0, IOR=3/
&DEVC ID='TSC_F_04', QUANTITY='INCIDENT HEAT FLUX', XYZ=-1.015,0.4,0.0, IOR=3/
&DEVC ID='TSC_F_05', QUANTITY='INCIDENT HEAT FLUX', XYZ=-1.265,0.4,0.0, IOR=3/
&DEVC ID='TSC_F_06', QUANTITY='INCIDENT HEAT FLUX', XYZ=-2.015,0.4,0.0, IOR=3/
&DEVC ID='TSC_F_07', QUANTITY='INCIDENT HEAT FLUX', XYZ=-1.765,0.4,0.0, IOR=3/
&DEVC ID='TSC_F_08', QUANTITY='INCIDENT HEAT FLUX', XYZ=-1.515,0.4,0.0, IOR=3/

&SLCF PBY=0.1, QUANTITY='TEMPERATURE' /
&SLCF PBY=0.2, QUANTITY='TEMPERATURE' /
&SLCF PBY=0.3, QUANTITY='TEMPERATURE' /
&SLCF PBY=0.4, QUANTITY='TEMPERATURE' /
&SLCF PBY=0.5, QUANTITY='TEMPERATURE' /
&SLCF PBY=0.6, QUANTITY='TEMPERATURE' /

&SLCF PBX=-0.16,QUANTITY='TEMPERATURE' /
&SLCF PBX=-0.6, QUANTITY='TEMPERATURE' /
&SLCF PBX=-1.2, QUANTITY='TEMPERATURE' /
&SLCF PBX=-1.8, QUANTITY='TEMPERATURE' /

&SLCF PBY=0.1, QUANTITY='VELOCITY', VECTOR = .TRUE. /
&SLCF PBY=0.2, QUANTITY='VELOCITY', VECTOR = .TRUE. /
&SLCF PBY=0.3, QUANTITY='VELOCITY', VECTOR = .TRUE. /
&SLCF PBY=0.4, QUANTITY='VELOCITY', VECTOR = .TRUE. /
&SLCF PBY=0.5, QUANTITY='VELOCITY', VECTOR = .TRUE. /
&SLCF PBY=0.6, QUANTITY='VELOCITY', VECTOR = .TRUE. /

&SLCF PBX=-0.16,QUANTITY='VELOCITY', VECTOR = .TRUE. /
&SLCF PBX=-0.6, QUANTITY='VELOCITY', VECTOR = .TRUE. /
&SLCF PBX=-1.2, QUANTITY='VELOCITY', VECTOR = .TRUE. /
&SLCF PBX=-1.8, QUANTITY='VELOCITY', VECTOR = .TRUE. /

&SLCF PBY=0.1, QUANTITY='VOLUME FRACTION', SPEC_ID='OXYGEN' /
&SLCF PBY=0.2, QUANTITY='VOLUME FRACTION', SPEC_ID='OXYGEN' /
&SLCF PBY=0.3, QUANTITY='VOLUME FRACTION', SPEC_ID='OXYGEN' /
&SLCF PBY=0.4, QUANTITY='VOLUME FRACTION', SPEC_ID='OXYGEN' /
&SLCF PBY=0.5, QUANTITY='VOLUME FRACTION', SPEC_ID='OXYGEN' /
&SLCF PBY=0.6, QUANTITY='VOLUME FRACTION', SPEC_ID='OXYGEN' /

&SLCF PBX=-0.16,QUANTITY='VOLUME FRACTION', SPEC_ID='OXYGEN' /
&SLCF PBX=-0.6, QUANTITY='VOLUME FRACTION', SPEC_ID='OXYGEN' /
&SLCF PBX=-1.2, QUANTITY='VOLUME FRACTION', SPEC_ID='OXYGEN' /
&SLCF PBX=-1.8, QUANTITY='VOLUME FRACTION', SPEC_ID='OXYGEN' /

&SLCF PBY=0.1, QUANTITY='VOLUME FRACTION', SPEC_ID='PROPANE' /
&SLCF PBY=0.2, QUANTITY='VOLUME FRACTION', SPEC_ID='PROPANE' /
&SLCF PBY=0.3, QUANTITY='VOLUME FRACTION', SPEC_ID='PROPANE' /
```

```
&SLCF PBY=0.4, QUANTITY='VOLUME FRACTION', SPEC_ID='PROPANE' /
&SLCF PBY=0.5, QUANTITY='VOLUME FRACTION', SPEC_ID='PROPANE' /
&SLCF PBY=0.6, QUANTITY='VOLUME FRACTION', SPEC_ID='PROPANE' /

&SLCF PBX=-0.16,QUANTITY='VOLUME FRACTION', SPEC_ID='PROPANE' /
&SLCF PBX=-0.6, QUANTITY='VOLUME FRACTION', SPEC_ID='PROPANE' /
&SLCF PBX=-1.2, QUANTITY='VOLUME FRACTION', SPEC_ID='PROPANE' /
&SLCF PBX=-1.8, QUANTITY='VOLUME FRACTION', SPEC_ID='PROPANE' /

&BNDF QUANTITY = 'WALL TEMPERATURE' /
&BNDF QUANTITY = 'BURNING RATE'     /
&BNDF QUANTITY = 'INCIDENT HEAT FLUX' /
&BNDF QUANTITY = 'GAUGE HEAT FLUX'  /
&BNDF QUANTITY = 'CONVECTIVE HEAT FLUX' /
&BNDF QUANTITY = 'RADIATIVE HEAT FLUX' /

&TAIL /
```